JOURNAL OF BACTERIOLOGY, Sept. 1987, p. 4154–4162
0021-9193/87/094154-09$02.00/0

Vol. 169, No. 9

Molecular Characterization of the *Escherichia coli* Enterobactin Cistron *entF* and Coupled Expression of *entF* and the *fes* Gene

GREGG S. PETTIS AND MARK A. McINTOSH*

Department of Microbiology, School of Medicine, University of Missouri-Columbia, Columbia, Missouri 65212

Received 3 February 1987/Accepted 9 June 1987

The *Escherichia coli entF* gene, which encodes the serine-activating enzyme involved in enterobactin synthesis, has been localized to a 4.7-kilobase-pair DNA fragment inserted in the vector pBR328. This recombinant molecule, pITS32, restored the ability of an *entF* mutant to grow on low-iron medium and to produce enterobactin. Examination of its translation products by minicell and electrophoretic analyses revealed a protein of approximately 160,000 daltons, which we identified as the EntF protein. A small DNA segment from pITS32 containing the translational start site for *entF* allowed the low constitutive expression of β-galactosidase when cloned (pITS301) upstream of the *lacZ* structural gene in the vector pMC1403. In contrast, a clone (pITS312) containing the identical *entF-lacZ* fusion and a larger region upstream of *entF* including the entire *fes* gene and extending into the *fepA* gene (whose transcription is in the opposite direction relative to *entF*) expressed β-galactosidase in high yet inducible amounts in response to fluctuations in the metabolic iron concentration. Transposon insertion mutations in the *fes* gene but not an insertion near the 5′ region of *fepA* in pITS312 reduced this high inducible expression to the low constitutive level seen for pITS301. These observations are most readily explained by the presence of a regulatory region located upstream of *fes* which mediates the iron-regulated expression of a transcript that includes the *fes* and *entF* genes.

Enteric bacteria such as *Escherichia coli* utilize highly specific iron-chelating systems for the essential task of iron acquisition. Included in these systems are low-molecular-weight, high-affinity iron-binding compounds termed siderophores and the specific membrane components involved in the retrieval of ferric siderophore complexes from the environment (36). The indigenous siderophore of *E. coli* and *Salmonella typhimurium* is a cyclic trimer of 2,3-dihydroxybenzoylserine and is known by the trivial names enterochelin (37) and enterobactin (40).

The enterobactin gene cluster, including the genes specific for its biosynthesis, for its outer membrane receptor, FepA, and for certain other transport functions, maps near min 13 on the *E. coli* chromosome (1). The genes *entC*, *entB*, and *entA* encode the enzymatic activities which convert the aromatic pathway intermediate chorismate to 2,3-dihydroxybenzoic acid (51). This precursor is then coupled to L-serine, in a series of poorly understood reactions catalyzed by the products of the *entD*, *entE*, entF, and *entG* genes, to form the siderophore molecule (28, 49). Evidence has been presented to suggest that these four enzymes form a multienzyme complex referred to as enterochelin synthetase (15); knowledge of the roles for the individual components of this complex is incomplete. It has been demonstrated, however, that the products of the *entE* and *entF* genes catalyze the activation of 2,3-dihydroxybenzoic acid and L-serine, respectively, via ATP-dependent PP_i exchange reactions, thereby preparing these molecules for the final stages of enterobactin synthesis (15, 50).

Other genes responsible for the uptake and processing of the ferric enterobactin complex include the *fepA* gene, which encodes the outer membrane receptor originally identified as an 81,000-dalton protein (18, 41), the *fepB* and *fepC* genes (39), whose products appear to be involved in periplasmic and cytoplasmic membrane transport of the complex, respectively, and the *fes* gene, which is responsible for the intracellular release of iron from ferric enterobactin (27).

The genetic organization of the enterobactin cluster was first analyzed by Mu-induced transposition of these genes onto the plasmid RP4 (25); this study provided a partial gene order of *entD*, *fes*, *entF*, *fep*, *ent(CA)GBE*. Transposon Tn*5* mutational analysis of cloned restriction fragments suggested the predominance of independent transcriptional units for these genes (26). The work of Fleming et al. (12), involving construction of gene fusions via the Mu d(Ap^r *lac*) vector (7), confirmed the presence of separate transcripts for the *fepA* and *entF* genes, while suggesting that the *entA* (*CGB*)*E* genes constitute an operon. More importantly, however, this study provided direct evidence for coordinated regulation of the enterobactin genes at the transcriptional level in response to the intracellular iron concentration. These results were in accordance with those of previous kinetics studies (23) which concentrated on the siderophore receptor. The mechanism for this coordinated regulation is not known, but it appears to be shared among genes for other iron uptake systems present in *E. coli*, including those for ferrichrome (19) and aerobactin (3). A *trans*-acting factor encoded by the *fur* gene at min 15.5 (2, 20) appears to play a role in the repression of these systems.

Subcloning experiments specific for the left end of the enterobactin region further defined the immediate gene order as *entD*, *fepA*, *fes*, and *entF* (8, 13). Protein analysis of pertinent subclones (13) revealed that FepA is first produced as an 84,000-dalton precursor, which is later cleaved to form the 81,000-dalton active receptor. The *fepA* gene has since been sequenced and its product shown to be a 723-amino-acid protein (79,908 daltons) with a 22-amino-acid leader peptide attached in its precursor form (29). Additionally, the product of the *fes* gene was shown to be a 44,000-dalton protein, while no protein product was detected for the *entD* gene (13). The product of the *entF* gene was described as a 115,000-dalton soluble protein (8).

* Corresponding author.

TABLE 1. *E. coli* strains, plasmids, and bacteriophage

Strain, plasmid, or phage	Relevant genotype or phenotype	Reference or source
E. coli strains		
MC4100	F⁻ *araD139* Δ(*lacIOPZYA*)*U169 rpsL thiA*	7
MC4160	Δ*recA* derivative of MC4100	This study
AB1515	*thi trpE purE proC leuB lacY mtl xyl rpsL azi tonA tsx supE*	10
AN42	*thi his proA argE pheA tyrA trp rpsL entD*	28
AN49	*thi his proA argE pheA tyrA trp rpsL entF*	28
AN90	*purE*⁺ *entD* derivative of AB1515 by P1 transduction from AN42	10
AN90-60	Δ*recA* derivative of AN90	This study
AN92	*proA argE pheA tyrA trp rpsL aroB* Mu immune	51
AN117	*purE*⁺ *entF* derivative of AB1515 by P1 transduction from AN49	Obtained from I. G. Young
AN117-60	Δ*recA* derivative of AN117	This study
AN272	*proA argE pheA tyrA trp rpsL aroB fes*; isolated from AN92 after treatment with NTG[a]	27
MM272	*purE*⁺ *fes* derivative of AB1515 by P1 transduction from AN272	This study
MM272-60	Δ*recA* derivative of MM272	This study
χ984	*minA minB pdxC purE his rpsL xyl ilv met*	14
W1485	F⁺	Obtained from *E. coli* Genetic Stock Center
JC10284	*srlR*::Tn*10 srlC srlD metB mtl gatC gatA malA xyl rpsL sup* Δ(*srlR-recA*)	11
Plasmids		
pMC1403	Ap[r]	6
pBR328	Ap[r] Tc[r] Cm[r]	45
pITS	See Fig. 1	This study
Bacteriophage λ1105	Km[r]	48

[a] NTG, *N*-Methyl-*N'*-nitro-*N*-nitrosoguanidine.

This study continues our molecular analysis of the enterobactin region by first detailing the isolation of the *entF* gene and identification of its gene product. Further subcloning procedures coupled with complementation and protein analyses allowed localization of the *entF* translational start site to within a small region. Cloning of this region next to a promoterless *lacZ* gene permitted us to measure the expression of β-galactosidase in response to iron concentration. Additional *entF-lacZ* derivatives provided evidence that under normal environmental circumstances, expression of *entF* may be under the control of its own low-level constitutive promoter; however, expression is dramatically increased under iron stress, and this induction is regulated by an iron-responsive regulatory region that appears to be located upstream of the *fes* gene.

MATERIALS AND METHODS

Bacterial strains, plasmids, and bacteriophage. All *E. coli* strains used in this report are described in Table 1. Derivatives of the vector pBR328 are designated pITS (for plasmids containing iron transport system genes) and are shown in Fig. 1. Plasmid constructions involving the vector pMC1403 (kindly provided by Malcolm J. Casadaban) are diagrammed in Fig. 3. The λ1105 vector containing the p*tac*–mini-*kan* insertion element was the kind gift of Nancy Kleckner via George Smith. P1 transduction experiments to transfer relevant genetic markers between strains were carried out by the method of Miller (34). *recA* deletion derivatives of each strain were constructed by isolating P1 transductants which carried the *srl*::Tn*10* and Δ*recA* markers from strain JC10284. Spontaneous loss of Tn*10* was selected on Bochner plates (5), and retention of the *recA* deletion mutation was screened by sensitivity to UV irradiation.

Media, chemicals, and enzymes. Tris-succinate minimal medium (31) containing 100 μM 2,2'-dipyridyl was used as the selective low-iron medium. The concentration of supplements added has been described previously (12, 32). L-broth (LB) (34) and nutrient broth (8 g of nutrient broth [Difco Laboratories], 5 g of NaCl per liter) were used as complete media. LB and MacConkey-lactose medium were made iron rich by the addition of 20 μM $FeSO_4$ and 10 mM sodium citrate, while the addition of 200 μM 2,2'-dipyridyl resulted in iron-deficient conditions. Antibiotics were used at the following final concentrations: ampicillin, 25 μg/ml; chloramphenicol, 30 μg/ml; tetracycline, 10 μg/ml; kanamycin, 50 μg/ml; and nalidixic acid, 20 μg/ml. Restriction enzymes were purchased from Bethesda Research Laboratories (Gaithesburg, Md.), International Biotechnologies, Inc. (New Haven, Conn.), New England Biolabs (Beverly, Mass.), and Promega Biotec (Madison, Wis.). T4 DNA ligase and DNA polymerase I large (Klenow) fragment were purchased from Boehringer Mannheim (Indianapolis, Ind.). T4 DNA polymerase and [α-^{32}P]dATP (800 Ci/mmol) were from Amersham Corp. (Arlington Heights, Ill.). Restriction endonucleases and T4 DNA ligase were used according to the conditions recommended by the supplier. Isopropyl-β-D-thiogalactopyranoside was purchased from Sigma Chemical Co. and used at 40 μg/ml. Rabbit anti-β-galactosidase antiserum and peroxidase-conjugated goat anti-rabbit immunoglobulin G were from Cappel Laboratories (Malvern, Pa.).

Plasmid isolation and transformation. Plasmids were isolated by the alkaline lysis procedure of Birnboim and Doly (4). Purification was completed by cesium chloride-ethidium bromide density gradient centrifugation (30). The procedure of Cohen et al. (9) was used for transformation of $CaCl_2$-treated bacterial cells.

Electrophoresis of DNA and protein. DNA was analyzed on horizontal agarose slab gels in TAE buffer (30). Proteins

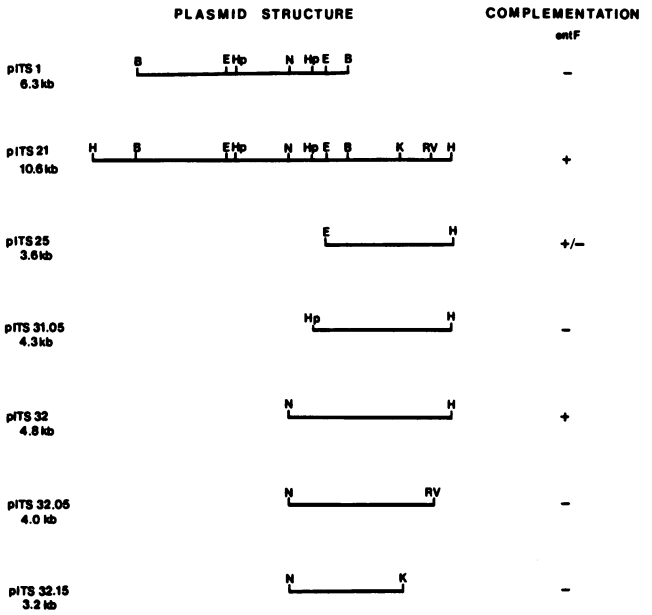

FIG. 1. Physical map of plasmids pITS1, pITS21, and derivatives. The horizontal lines refer to the *ent* region insert DNA cloned into the corresponding sites of pBR328 (pITS1, pITS21, and pITS25). The pITS31.05 *Hpa*I-*Hin*dIII insert was cloned into *Sph*I-*Hin*dIII-restricted pBR328 which had been blunt-ended at its *Sph*I end with T4 DNA polymerase prior to ligation. The *Nru*I-*Hin*dIII insert of pITS32 was cloned into pBR328 digested with *Eco*RV and *Hin*dIII. The clones pITS32.05 and pITS32.15 were made by deleting the small *Eco*RV-*Hin*dIII and *Kpn*I-*Hin*dIII fragments of pITS32, respectively. The pITS1 insert has been described previously (13). Fragment sizes are given in kilobases. Sites for (B) *Bam*HI, (E) *Eco*RI, (H) *Hin*dIII, (Hp) *Hpa*I, (K) *Kpn*I, (N) *Nru*I, and (RV) *Eco*RV are shown. Complementation was determined by the ability of the specified plasmids to allow AN117-60 (*entF*) transformants to grow on low-iron medium and to produce enterobactin as detected by bioassay (12). Symbols: +, strong complementation; +/−, weak complementation; −, no complementation.

were separated on vertical sodium dodecyl sulfate (SDS)–7.5% polyacrylamide gels in 3% urea by the method of Laemmli (24). Samples were boiled for 5 min in sample buffer (62.5 mM Tris hydrochloride, pH 6.8, 2% SDS, 5% 2-mercaptoethanol, 10% [vol/vol] glycerol, 3% urea, 0.001% bromophenol blue) prior to loading. Proteins were visualized with Coomassie brilliant blue R-250 and [^{35}S]methionine labeled polypeptides were detected by autoradiography on Kodak XAR-2 film.

Construction of in-phase *entF-lacZ* gene fusions. The 0.5-kilobase-pair (kb) *Nru*I-*Hpa*I and the 2.0-kb *Hpa*I fragments of pITS21 were isolated from 0.7% low-melting-point agarose gels. These blunt-ended DNA fragments were ligated into *Sma*I-digested pMC1403. Prior to transformation of strain MC4160, ligation mixes were digested with *Sma*I to minimize transformation by nonrecombinant vector molecules. Ampicillin-resistant (Amp^r) clones appearing on LB were checked for the presence of recombinant plasmids. Plasmid DNA was isolated and inserts were identified and checked for correct orientation by restriction mapping. Clones containing properly oriented inserts (pITS300 and pITS311) were tested for iron-regulated β-galactosidase expression by replica plating onto low- and high-iron MacConkey lactose medium and then by assaying for β-galactosidase activity. The lack of β-galactosidase expression for either clone was assumed to be due to the *lacZ* sequence being out of phase with respect to the reading frame of the upstream *entF* sequence, resulting in the production of a nonsense protein. Frameshift mutations to correct the reading frame were generated by using the *Bam*HI site just downstream of the *Sma*I cloning site in the vector pMC1403. The recombinant plasmids were digested with *Bam*HI at the junction of the *entF* and *lacZ* sequences, and the ends were filled in with Klenow fragment to create a 4-base insertion and therefore a 1-base frameshift reading into the *lacZ* sequence. The plasmids were then religated and subsequently used to transform MC4160. Amp^r clones appearing on LB were checked for iron-regulated β-galactosidase expression as described above. A number of positive clones were picked, and their plasmid DNA was isolated and then subjected to restriction analysis to verify that all Lac$^+$ clones had lost their *Bam*HI sites.

Immunological detection of EntF-LacZ hybrid proteins. Cultures were grown to mid-log phase in LB made iron rich or iron poor as described above. Cells were harvested and suspended in sample buffer prior to boiling. Proteins were separated by electrophoresis as described above and transferred to nitrocellulose paper by the method of Towbin et al. (46). The blot was incubated for 1 h at 37°C with rabbit anti-*E. coli*-β-galactosidase antiserum diluted 1:1,000 in 0.9% NaCl–10 mM Tris (pH 7.4)–1.5% bovine serum albumin. After being washed, the blot was treated with peroxidase-conjugated goat anti-rabbit immunoglobulin G and developed with 4-chloro-1-naphthal as a substrate (21).

β-Galactosidase assay. The method of Miller (34) was used to assay the β-galactosidase activity of chloroform-treated cells grown in LB under various iron conditions.

Tn*1000* and p*tac*–mini-*kan* mutagenesis. Recombinant plasmids were mutagenized with Tn*1000* by the procedure described by Guyer (17). Briefly, strain MC4160(pITS312) was made F$^+$ by mating with strain W1485. The recombinant plasmid could then be mobilized by the F plasmid containing Tn*1000* during mating with the recipient MC4160 (Nal^r) in a 1:1 donor-to-recipient ratio. Amp^r Nal^r transconjugants growing on low-iron MacConkey-lactose medium were screened for the presence of Tn*1000* by the published restriction map (16). Selected clones were then assayed for β-galactosidase activity and screened for Fes$^+$ activity by their ability to restore efficient growth on nutrient broth when transformed into MM272-60 (Fes$^-$).

For mutagenesis with the p*tac*–mini-*kan* element (48), MC4160(pITS312) was infected with λ1105 at a multiplicity of 1. Cells were diluted into LB and grown in the presence of high (300 μg/ml) kanamycin; plasmid DNA was isolated and used to transform MC4160, and Amp^r Kan^r transformants were selected on LB agar. Insertions were mapped with restriction endonucleases, and individual clones were evaluated for their β-galactosidase and Fes$^+$ activities as described above.

DNA sequencing. Fragments specific for both strands of the 493-base-pair (bp) *Nru*I-*Hpa*I region containing the translational start site of *entF* were cloned into bacteriophage M13 mp18 and mp19 derivatives, and single-strand template was isolated (33). Nucleotide sequences were determined by the dideoxy chain termination method of Sanger et al. (43). The junction sequences of the various *entF-lacZ* pMC1403 derivatives were sequenced by the dideoxy technique; a primer initiating from the 5′ *lacZ* sequence was annealed to fusion-containing templates and extended with Klenow fragment through the polylinker region, across the fusion junction, and approximately 50 bases into the insert fragment.

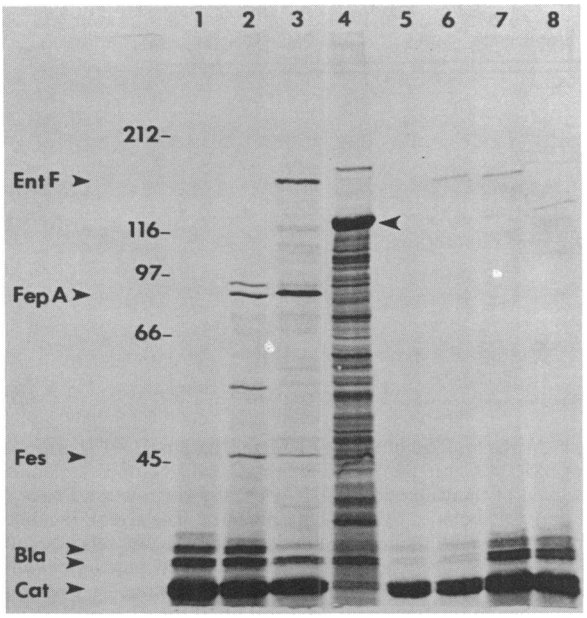

FIG. 2. Autoradiogram of ^{35}S-labeled proteins expressed from plasmid-containing minicells. Strain χ984 was transformed with the specified plasmids (see Fig. 1), and minicells were isolated as described (14). Minicell preparations were labeled for 60 min with 1 mCi of [^{35}S]methionine per ml at 37°C under iron-limiting conditions (13), washed with cold medium, and boiled for 5 min in sample buffer. Labeled proteins were separated on a 7.5% polyacrylamide–3% urea gel in the presence of SDS and visualized by exposing the dried gel to KODAK XAR-2 film for 24 h. The positions of enterobactin-related gene products (EntF, FepA, and Fes), β-lactamase (Bla), and CAT are shown, and the arrow in lane 4 indicates a CAT-EntF fusion product. Lanes: 1, pBR328; 2, pITS1; 3, pITS21; 4, pITS25; 5, pITS31.05; 6, pITS32; 7, pITS32.05; 8, pITS32.15. Molecular mass markers are indicated in kilodaltons.

RESULTS

In vitro cloning and complementation of the *entF* gene. Cloning of the 6.3-kb *Bam*HI fragment, which encodes the structural genes *entD*, *fes*, and *fepA*, into the *Bam*HI site of the vector pBR328 was described previously (13). The 0.6-kb *Eco*RI-*Bam*HI segment of this insert was isolated from low-melting-point agarose (30) and labeled by nick translation (42) for use as a probe against a complete *Hin*dIII *E. coli* chromosomal digest. A band of approximately 10 kb was recognized. Fragments in this size range were isolated from a preparative 0.7% low-melting-point agarose gel and ligated into *Hin*dIII-digested pBR328. Upon transformation of strain HB101, all Tet^s Cam^r Amp^r colonies were pooled, and the recombinant plasmid DNA was isolated.

To identify clones relevant to our studies, this partial library was used to transform the *entD* mutant AN90-60. Colonies appearing on Tris-succinate medium containing chloramphenicol represented clones capable of growth under iron-deficient conditions due to enterobactin production. Isolation of plasmid DNA from one of these clones and subsequent transformation of AN90-60 confirmed the presence of the EntD$^+$ activity. We then investigated this recombinant plasmid, pITS21, for its ability to complement known enterobactin biosynthesis and transport activities following transformation into relevant *ent recA* double mutants. Complementation for *entD*, *fes*, and *fepA* genes was done as described previously (13). The presence of the *entF* gene was established by restoration of low-iron growth and enterobactin-producing capabilities to the *entF* mutant strain AN117-60. Physical characterization of the cloned insert of pITS21 confirmed that it was identical to the 10.6-kb *Hin*dIII fragment corresponding to the left end of the enterobactin cluster isolated by Laird et al. (25) and described further by Coderre and Earhart (8).

Restriction analysis and subcloning of pITS21. Previous studies of the 6.3-kb *Bam*HI fragment contained within pITS21 (Fig. 1) defined the location of the *entD*, *fes*, and *fepA* genes (13). Further analysis was performed on pITS21 to orient the *entF* gene with relation to the other loci. Standard mapping techniques with many different restriction enzymes produced a detailed physical map of the 10.6-kb *Hin*dIII insert of pITS21. EntF$^+$ activity was localized to the 4.7-kb *Nru*I-*Hin*dIII fragment of pITS32. The absence of EntF activity in pITS31.05 and pITS32.05 localized the left end of *entF* between the *Nru*I and *Hpa*I sites and the right end between the *Eco*RV and *Hin*dIII sites. The partial EntF$^+$ activity of the 3.6-kb *Eco*RI-*Hin*dIII insert of pITS25 was intriguing and suggested that the activity may be due to the production of a fusion protein consisting of the amino terminus of chloramphenicol acetyltransferase (CAT) fused in phase to the carboxy terminus of the EntF protein. This assumption was confirmed in the translational studies discussed below. Together, the subcloning data supported the previous observation that *entF* is transcribed from left to right (12).

Identification of the EntF protein in minicells. The clone pITS1 has already been shown to encode the FepA receptor protein, along with its precursor, and the 44,000-dalton Fes protein (13). To identify the *entF* product, the minicell strain χ984 was transformed with pITS21 and its derivatives. The electrophoretic migration patterns of labeled proteins specific for these plasmids, including pITS1, are shown in Fig. 2. A comparison of the profile of pITS21 with that of pITS1 revealed the additional expression of a high-M_r band of approximately 160,000. This represented the full-length EntF protein which was also present in the *entF*-specific subclone pITS32 and corresponded to the EntF protein originally described as being 115,000 daltons (8). The 54,000-dalton protein seen for pITS1 was previously suggested to arise from a promoter located in the 0.6-kb *Bam*HI-*Eco*RI fragment reading out into vector sequences (13). This polypeptide can now be identified as a truncated EntF protein, with the location of its amino terminus confirmed by the proteins expressed from subclones pITS25 and pITS31.05. The partial *entF* clone pITS25 strongly expressed a truncated version of the EntF protein at 120,000 daltons, along with an intense background of cellular protein contamination. Due to its size and relative abundance, it appears that the truncated EntF was the result of an in-phase fusion between the amino-terminal portion of the CAT protein (and was therefore directed by the strong *cat* gene promoter) and the partially functional carboxyl 80% of the *entF* product. The overproduction of this abnormal protein appeared to be somewhat toxic to the minicell strain, in that cells appeared more filamented than usual, yielding extremely low amounts of minicells relative to χ984 containing any of the other plasmids tested. This limited the extent of minicell purification for pITS25. The profile for pITS31.05, whose insert region spanned that of pITS25 but was not cloned adjacent to the *cat* promoter, displayed no iron-related proteins. This provided evidence that the translational initiation site of *entF* lay upstream of the *Hpa*I site, within the insert region of pITS32. The remaining profiles for pITS32.05 and

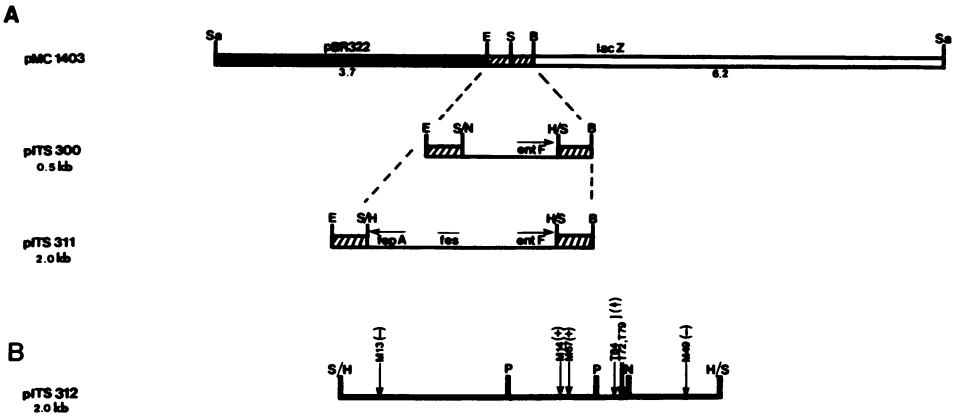

FIG. 3. (A) Construction of *entF-lacZ* gene fusion plasmids. The 0.5-kb *Nru*I-*Hpa*I (middle line) and the 2.0-kb *Hpa*I (bottom line) fragments from pITS21 were blunt-end ligated into the *Sma*I site of the vector pMC1403 (top line) to create the specified clones. Orientations were verified by restriction mapping. These plasmids were subsequently cleaved at their unique *Bam*HI sites, the single-strand ends were filled in with Klenow fragment, and the plasmids were religated to create the derivative clones pITS301 and pITS312. The size of the inserted DNA fragment is given (in kilobases) under each specified plasmid name. Transcriptional directions are indicated by arrows. (B) Location of Tn*1000* and p*tac*–mini-*kan* insertions in the *ent* region of pITS312. pITS312 was mutagenized with Tn*1000* (T) and p*tac*–mini-*kan* (M) transposable elements as described in the text, and the location and orientation of individual insertions were determined by restriction cleavage site mapping. The symbols + and − indicate the two possible orientations in relation to an arbitrary point for each p*tac*–mini-*kan* element inserted into pITS312; the horizontal, leftward pointing arrow represents the single observed orientation in relation to an arbitrary point for all Tn*1000* polar insertions in pITS312. Abbreviations: B, *Bam*HI; E, *Eco*RI; H, *Hpa*I; H/S, *Hpa*I/*Sma*I hybrid site; N, *Nru*I; P, *Pvu*I; S, *Sma*I; Sa, *Sal*I; S/H, *Sma*I/*Hpa*I hybrid site; S/N, *Sma*I/*Nru*I hybrid site.

pITS32.15, both of which lacked EntF$^+$ activity and expressed slightly truncated EntF proteins, suggested that the gene must extend to just beyond the *Eco*RV site. DNA sequence analysis confirmed this observation by revealing that the EntF protein encoded by pITS32.05 was truncated by some 30 amino acids at its carboxyl end (data not shown). The lack of activity when the EntF protein was truncated even slightly at the *Eco*RV site emphasized the importance of the carboxy terminus for proper enzymatic function.

Construction of *entF-lacZ* gene fusions. To investigate the iron-mediated regulation of *entF* expression, gene fusions to a promoterless *lacZ* gene were constructed. The 0.5-kb *Nru*I-*Hpa*I fragment containing the translational start of *entF* was ligated into the *Sma*I site adjacent to *lacZ* in the vector pMC1403 (6). The resulting clone, pITS300 (Fig. 3A), was determined by restriction mapping to contain the desired insert in the correct orientation. Strain MC4160 (pITS300) was tested for an iron-regulated Lac$^+$ phenotype on both low- and high-iron MacConkey-lactose medium and in assays for β-galactosidase activity, but no activity was detected (Table 2). This suggested that in the gene fusion construction, the *lacZ* sequence was not being read in the proper frame, resulting in a nonsense protein. To create a 1-base frameshift reading into the *lacZ* sequence, pITS300 was digested with *Bam*HI at the *entF-lacZ* junction, and the ends were filled in with Klenow fragment and then ligated. Strain MC4160 transformants were identified as being Lac$^+$ on low-iron MacConkey medium. The plasmids of several Lac$^+$ clones were verified as having lost their *Bam*HI sites by restriction mapping. This frameshift fusion plasmid, pITS301, displayed low constitutive β-galactosidase expression in assays of cells grown under both high- and low-iron conditions (Table 2), which indicated that the iron-responsive sequence controlling *entF* expression was located upstream of the *Nru*I site.

To localize this regulatory region, a clone was constructed which contained the identical *entF-lacZ* fusion (so that comparative hybrid protein stability would not be a factor) but also a much larger upstream region. Transposon mutagenesis of this plasmid would then serve to define regions critical to the iron-mediated expression of the hybrid protein. The 2.0-kb *Hpa*I fragment, shown in its desired orientation in Fig. 3A, not only spanned the entire *fes* gene but extended into the *fepA* gene (29), which is known to be transcribed in the opposite direction relative to *entF* (12). This fragment was isolated and cloned into the *Sma*I site of pMC1403. The correctly oriented insert (pITS311) was identified by restriction mapping. This clone, like pITS300, displayed no β-galactosidase activity in assays done under various iron concentrations (Table 2). However, upon creation of a frameshift at the *Bam*HI site, the new clone, pITS312, exhibited high yet inducible expression of β-galactosidase (Table 2). The units, an approximately fivefold

TABLE 2. β-Galactosidase activity in response to iron concentration by *entF-lacZ* gene fusion plasmids[a]

Plasmid	Fes activity[b]	β-Galactosidase activity[c] (U)	
		With Fe	Without Fe
pITS300	−	0	0
pITS301	−	23	27
pITS311	+	0	0
pITS312	+	227	1,579
pITS312-T12	+	489	1,650
pITS312-T72	−	15	12
pITS312-T79	−	1	0
pITS312-T84	−	14	13
pITS312-M13	+	229	1,551
pITS312-M14	−	2	10
pITS312-M49	+	31	47
pITS312-M67	−	0	0

[a] Strain MC4160 or a related derivative was used as the host for all β-galactosidase assays.

[b] Fes activity was determined by the ability of MM272-60 transformants to grow efficiently on nutrient broth medium.

[c] The values represent the mean of three independent β-galactosidase assays for each strain.

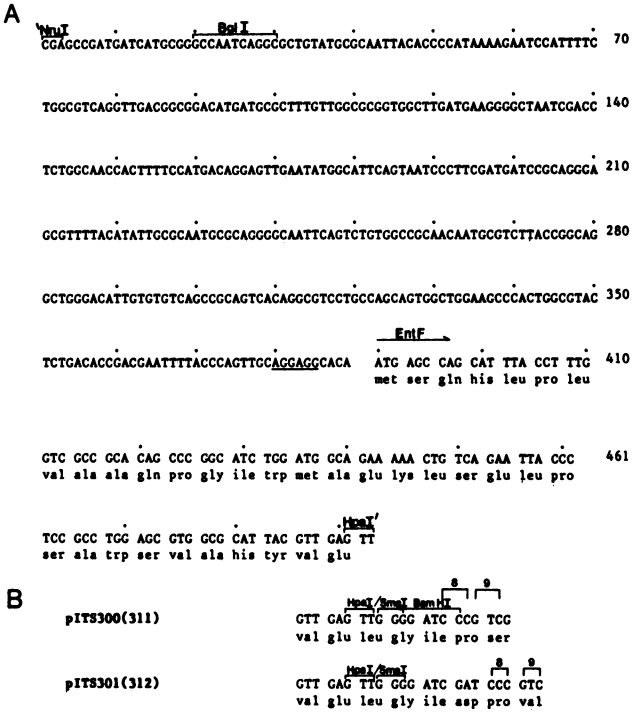

FIG. 4. (A) Nucleotide sequence of the 493-bp *Nru*I-*Hpa*I insert region. DNA sequencing was performed as described in the text. A consensus Shine-Dalgarno ribosome-binding region (44) is underlined and precedes by 5 bp the proposed translation initiation site for *entF*. The corresponding amino-terminal amino acids for the EntF protein are listed under the proposed coding sequence. Only the coding strand for *entF* is given. '*Nru*I, 3' one-half of the *Nru*I restriction site generated by digestion with this enzyme; *Hpa*I', 5' one-half of the *Hpa*I restriction site generated by digestion with this enzyme. (B) Junction sequences of the various *entF-lacZ* fusion constructs. The sequences shown consist of the *Nru*I-*Hpa*I insert at its 3' end nucleotides and the adjacent polylinker region that remains flanked by the 5' *lacZ* sequence upon creation of these pMC1403 derivatives. Only the coding strand is shown. The reading frame is that established by the upstream translation start of *entF*. The corresponding amino acid is given below each codon. The hybrid *Hpa*I/*Sma*I restriction site, the result of cloning the 5' end of the *Hpa*I site of the insert fragment adjacent to the 3' end of the *Sma*I site of the vector, is indicated, as is the complete *Bam*HI site which is present only in clones pITS300 and pITS311. The eighth and ninth codons of *lacZ* in pMC1403 are bracketed.

increase in both high- and low-iron conditions over those seen for a Mu d(Ap^r *lac*) fusion into the chromosomally located *entF* gene (12), are presumably a reflection of the multicopy state of the plasmid.

To ensure that none of the fusion genes studied were phenotypically altered due to a cloning artifact, the constructs were examined for their nucleotide sequences in the *entF*-specific insert region and adjoining *entF-lacZ* junctions. Figure 4A displays the complete sequence of the 493-bp *Nru*I-*Hpa*I insert fragment common to all of the fusion constructs and shown by subcloning and protein analysis to contain the translational start site of *entF*. Analysis of this sequence suggested that the most likely site for this initiation was the ATG beginning at base 390. This putative start allowed an open reading frame of 104 bp extending to the *Hpa*I site and was preceded 5 bp upstream by a consensus Shine-Dalgarno ribosome-binding region (44). Examination of the junction sequences (Fig. 4B) of the various fusion constructs provided confirmation that this reading frame was pertinent to *entF* translation. Cloning of the *entF* coding region immediately upstream of *lacZ* produced the nonexpressing fusions pITS300 and pITS311 as a result of the *lacZ* sequence being out of phase with respect to the codon recognition specified by the proposed *entF* translation start. However, when the *Bam*HI site at the *entF-lacZ* junction was extended by 4 bp to create the expressing clones pITS301 and pITS312, the *lacZ* sequence was properly recognized by the same reading frame. Without a partial sequence of the EntF protein we cannot at this time dismiss the possibility that the *entF* coding region begins elsewhere yet is still aligned with this *lacZ* reading frame. However, all other possible start sites within this context were characterized by much less conserved translational signals. Nonetheless, it is clear from these data that the difference in expression seen between pITS301 and pITS312 was not an artifact of the fusion construction and must have arisen from the inclusion of an iron-responsive region upstream of the *entF-lacZ* fusion of pITS312.

Localization of the iron-responsive regulatory region for *entF*. To determine the location of the iron-regulated sequence controlling expression of the *entF-lacZ* gene fusion in pITS312, mutagenesis with Tn*1000* and the p*tac*–mini-*kan* insertion element (48) was performed. A shift from the high inducible β-galactosidase response of pITS312 to a lower level of expression similar to that of pITS301 would indicate insertions positioned either in this regulatory region or between this element and the *entF-lacZ* fusion. Following Tn*1000* mutagenesis, MC4160(pITS312) cells containing random insertions on the plasmid were plated on low-iron MacConkey-lactose medium. Both larger red colonies and smaller white colonies were seen. Clones representative of both phenotypes were screened for the position and orientation of their Tn*1000* insertions based on the restriction map provided by Guyer (16). Those containing a copy of Tn*1000* within the insert region (Fig. 3B) were also tested for Fes$^+$ activity as described earlier and assayed for β-galactosidase expression in response to iron (Table 2). Three insertion mutants (pITS312-T72, -T79, and -T84) lacked Fes$^+$ activity due to insertion of Tn*1000*, and expression of the hybrid EntF-LacZ protein was nearly eliminated or reduced from the inducible levels of pITS312 to a low constitutive level similar to pITS301. The fourth mutation (pITS312-T12) was located in the vector, not *fes*, and had no effect on expression of the fusion protein.

Further mutagenesis with the p*tac*–mini-*kan* insertion element yielded additional insertions (Fig. 3B) which mapped both in *fes* and between this gene and the *entF-lacZ* fusion. Again, as shown in Table 2, insertions (pITS312-M14 and -M67) in *fes* and an insertion (pITS312-M49) which mapped just downstream of *fes* severely reduced or eliminated expression of the hybrid EntF-LacZ protein. In contrast, an insertion (pITS312-M13) which mapped near the 5' end of the *fepA* gene in the insert region did not alter the expression pattern noted for pITS312. The small variations in expression noted between these insertion mutants are probably not solely attributable to direct effects of the transposons themselves. The three Tn*1000* insertions, for example, were all in a single orientation, mapped in a cluster, and yet showed a range from 0 to 15 U of β-galactosidase activity. Therefore, it is not clear whether this range of activity is merely the background level of the enzyme or is due to a possible low-level promoter between the insertion sites and the *entF-lacZ* fusion junction. Together, these mutagenesis studies indicate that the iron-

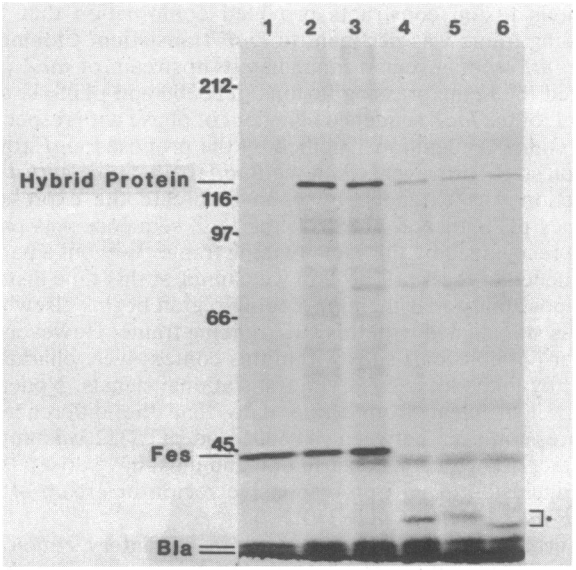

FIG. 5. Autoradiogram of ^{35}S-labeled proteins expressed by gene fusion plasmids. Strain χ984 was transformed with various *entF-lacZ* fusion constructs, minicells were isolated (14), and proteins were prepared and separated as described in the legend to Fig. 2. The asterisk denotes truncated Fes products due to insertion of Tn*1000*. Lanes: 1, pITS311; 2, pITS312; 3, pITS312-T12; 4, pITS312-T72; 5, pITS312-T79; 6, pITS312-T84. Molecular mass standards are indicated in kilodaltons.

responsive region controlling expression of the *entF-lacZ* fusion is located between insertions M13 and M14 in pITS312, with the most plausible position being somewhere upstream of the *fes* gene yet not extending into the *fepA* region. This infers that both *fes* and *entF* are included on an inducible mRNA that is transcribed in a clockwise direction beginning upstream of *fes*.

To demonstrate further the effects of these insertions, all fusion plasmids were transformed into strain χ984 to observe their protein profiles. pITS311 expressed only the 44,000-dalton Fes protein, whereas its frameshift derivative pITS312 expressed both Fes and a protein of 120,000 daltons, which represented the hybrid EntF-LacZ protein (Fig. 5). The expression of these proteins was unaffected by the Tn*1000* insertion (pITS312-T12) located in the vector; however, the remaining Tn*1000* insertions, all located in the *fes* gene, resulted in various truncated versions of Fes and appeared to reduce the amount of the full-length hybrid protein produced in this system. Similar results were obtained with the p*tac*–mini-*kan* derivatives of pITS312 (data not shown). We were unable to detect production in minicells of this same hybrid protein for pITS301 despite the low constitutive expression measured in β-galactosidase assays with this clone. Although the basis for this ambiguity is unknown, others (38) have noted the often unpredictable nature of protein expression in minicells. We therefore sought a more reliable and controlled system in which hybrid protein expression would mimic that functionally detected in β-galactosidase assays. Strain MC4160 containing various *entF-lacZ* fusion vectors was grown in LB (made iron rich or iron poor) to mid-log phase and harvested, and proteins were prepared and electrophoresed as described above. These were transferred to nitrocellulose paper (46) and reacted with antiserum raised against purified *E. coli* β-galactosidase. In this detection system, a single protein of M_r 120,000 was identified for both pITS301 and pITS312 (data not shown), confirming the identification of this product as the EntF-LacZ hybrid protein.

DISCUSSION

Isolation of the *entF* gene allowed unambiguous identification of its gene product. The recombinant subclone pITS32 yielded an EntF protein which, under the conditions used, had an apparent molecular weight of 160,000. This size is somewhat higher than that previously reported, 115,000, which was determined under different electrophoresis conditions (8). Based on subcloning and complementation data, the *entF* coding region spans somewhat less than 4 kb of DNA, implying that the actual molecular weight of the protein product is closer to 140,000. DNA sequence analysis of the *entF* region will allow precise size determination for both the gene and gene product.

It has been determined in this report that the extreme carboxy terminus of EntF is critical for proper enzymatic function, since a slight truncation of this end as seen in pITS32.05 resulted in a measurable loss of activity. A rather surprising complementation result was revealed for pITS25, which coded for a truncated EntF protein of M_r 120,000 having approximately 20% of its amino terminus replaced by the first 71 amino acids of the CAT protein. An *entF* mutant strain containing this plasmid displayed a weak ability to grow on low-iron medium and to produce enterobactin. Although it is possible that the hybrid protein itself is entirely responsible for the observed complementation results, it is tempting to speculate that the large EntF enzyme exists as a multimer comprising separate enzymatic domains which may function in concert so that individual molecules can contribute to the overall enzymatic activity. This is reminiscent of another large *E. coli* enzyme, β-galactosidase, in which enzymatic domains may be contributed to by separate protein molecules (47), a phenomenon known as α-complementation. In the instance described here, the portion of the EntF enzyme which was deleted in the construction of the CAT-EntF fusion in pITS25 may be provided by the chromosomally encoded *entF* gene, which must then be mutated somewhat downstream of the fusion junction.

Subcloning and complementation analyses of the *entF* region allowed us to localize the translational start site to within a 493-bp *Nru*I-*Hpa*I DNA fragment. When cloned in phase with the *lacZ* structural gene (pITS301), this segment permitted low constitutive expression of the fusion protein as measured by β-galactosidase activity. After addition of sequences extending upstream through the *fes* gene and into the 5′ region of the *fepA* gene (pITS312), this same hybrid protein was expressed in an inducible manner in response to iron. These data indicated that the iron-responsive regulatory region for *entF* is not contained within pITS32 and thus explain why complementation results for pITS32 were never as strong as those for pITS21 (G. Pettis, unpublished results). Tn*1000* and p*tac*–mini-*kan* insertions both between *fes* and the *entF-lacZ* fusion and into the *fes* gene, resulting in truncation of its gene product, had a polar effect on expression of the hybrid protein in pITS312; the original high yet iron-inducible response was now eliminated or reduced to the low constitutive level seen with pITS301. In contrast, a transposon insertion located near the start of the *fepA* gene had no effect on the normal expression levels of pITS312. These results indicated that a regulatory region located between the *fes* and *fepA* genes is required for the iron-

inducible expression of a transcript that includes the *fes* and *entF* genes. We cannot entirely exclude the less likely possibility that an iron-responsive region located within *fes* and at least some 700 bp upstream of the proposed translational start site of *entF* is responsible for inducible *entF* expression.

The low constitutive β-galactosidase expression of pITS301, as well as the rather limited *entF* complementation ability of pITS32, may be due to a promoter situated either in *fes* (whose coding region appears to span the *Nru*I site in pITS21; G. Pettis, unpublished results) or downstream of this gene that is specific for *entF* and which under normal conditions functions to allow a low yet constant supply of this serine-activating enzyme for use in other cellular metabolic pathways in addition to enterobactin synthesis. Enzymes with similar function have, for example, been shown to be integral components of antibiotic synthetase systems of *Bacillus* spp. (22) and are likely to be involved in the production of the peptide phytotoxin syringotoxin from strains of *Pseudomonas syringae* pv. *syringae* (35). However, the possibility that the low activity of pITS301 and the polar transposon insertion mutants of pITS312 reflects only residual nonspecific expression of *entF* cannot be dismissed, since a basal level of expression under high-iron conditions was detected for all enterobactin genes examined during earlier Mu d(Ap^r *lac*) fusion studies (12). It is also possible that the 493-bp *Nru*I-*Hpa*I insert portion of pITS32 and pITS301 provides only the translational start signals and 5′ *entF* coding sequence, while the actual promoter function is derived from upstream vector sequences. An analysis of the region immediately upstream of the proposed *entF* translational start site (Fig. 4A) revealed no strong canonical promoter determinants. Only qualitative and quantitative S1 mapping of all prospective transcription start sites for *fes* and *entF* will confirm their existence and possible roles in the regulatable expression of these genes.

Fusion constructions similar to those described here will allow us to compare the location of the regulatory region controlling expression of the *fepA* gene with that of the region mediating production of the polycistronic transcript that includes the *fes* and *entF* genes. Mutational analysis of this intergenic region should then reveal whether these regulatory elements exist independently or have some common sequences.

ACKNOWLEDGMENTS

We thank D. Pintel, K. Wise, and T. Fleming for helpful discussions during the course of these studies. We are especially grateful to A. J. Clark, M. Casadaban, I. G. Young, and B. Bachmann for providing bacterial strains and to G. Smith and N. Kleckner for providing λ1105. Our special thanks to K. Ehlert for preparation of the manuscript.

This work was supported by grants PCM 8210415 and DMB 8416017 from the National Science Foundation. G.S.P. is the recipient of a predoctoral traineeship from the National Institute of General Medical Sciences (5 T32 GM07494).

LITERATURE CITED

1. **Bachmann, B. J.** 1983. Linkage map of *Escherichia coli* K-12, edition 7. Microbiol. Rev. **47**:180–230.
2. **Bagg, A., and J. B. Neilands.** 1985. Mapping of a mutation affecting regulation of iron uptake systems in *Escherichia coli* K-12. J. Bacteriol. **161**:450–453.
3. **Bindereif, A., and J. B. Neilands.** 1985. Promoter mapping and transcriptional regulation of the iron assimilation system of plasmid ColV-K30 in *Escherichia coli* K-12. J. Bacteriol. **162**: 1039–1046.
4. **Birnboim, H. C., and J. Doly.** 1979. A rapid alkaline extraction procedure for screening recombinant plasmid DNA. Nucleic Acids Res. **7**:1513–1523.
5. **Bochner, B. R., H. Huang, G. L. Schieven, and B. N. Ames.** 1980. Positive selection for loss of tetracycline resistance. J. Bacteriol. **143**:926–933.
6. **Casadaban, M. J., J. Chou, and S. N. Cohen.** 1980. In vitro gene fusions that join an enzymatically active β-galactosidase segment to amino-terminal fragments of exogenous proteins: *Escherichia coli* plasmid vectors for the detection and cloning of translational initiation signals. J. Bacteriol. **143**:971–980.
7. **Casadaban, M. J., and S. N. Cohen.** 1979. Lactose genes fused to exogenous promoters in one step using a Mu-*lac* bacteriophage: in vivo probe for transcriptional control sequences. Proc. Natl. Acad. Sci. USA **76**:4530–4533.
8. **Coderre, P. E., and C. F. Earhart.** 1984. Characterization of a plasmid carrying the *Escherichia coli* K-12 *entD*, *fepA*, *fes* and *entF* genes. FEMS Microbiol. Lett. **25**:111–116.
9. **Cohen, S. N., A. C. Y. Chang, and L. Hsu.** 1972. Nonchromosomal antibiotic resistance in bacteria: genetic transformation of *Escherichia coli* by R-factor DNA. Proc. Natl. Acad. Sci. USA **69**:2110–2114.
10. **Cox, G. B., F. Gibson, R. K. J. Luke, N. A. Newton, I. G. O'Brien, and H. Rosenberg.** 1970. Mutations affecting iron transport in *Escherichia coli*. J. Bacteriol. **104**:219–226.
11. **Csonka, L. N., and A. J. Clark.** 1979. Deletions generated by the transposon Tn*10* in the *srl recA* region of the *Escherichia coli* K-12 chromosome. Genetics **93**:321–343.
12. **Fleming, T. P., M. S. Nahlik, and M. A. McIntosh.** 1983. Regulation of enterobactin iron transport in *Escherichia coli*: characterization of *ent*::Mu *d*(Ap^r *lac*) operon fusions. J. Bacteriol. **156**:1171–1177.
13. **Fleming, T. P., M. S. Nahlik, J. B. Neilands, and M. A. McIntosh.** 1985. Physical and genetic characterization of cloned enterobactin genomic sequences from *Escherichia coli* K-12. Gene **34**:47–54.
14. **Frazer, A. C., and R. Curtiss III.** 1975. Production, properties and utility of bacterial minicells. Curr. Top. Microbiol. Immunol. **69**:1–84.
15. **Greenwood, K. T., and R. K. J. Luke.** 1976. Studies on the enzymatic synthesis of enterochelin in *Escherichia coli* K-12: four polypeptides involved in the conversion of 2,3-dihydroxybenzoate to enterochelin. Biochim. Biophys. Acta **454**:285–297.
16. **Guyer, M. S.** 1978. The γδ sequence of F is an insertion sequence. J. Mol. Biol. **126**:347–365.
17. **Guyer, M. S.** 1983. Uses of the transposon γδ in the analysis of cloned genes. Methods Enzymol. **101**:362–369.
18. **Hancock, R. E. W., K. Hantke, and V. Braun.** 1976. Iron transport in *Escherichia coli* K-12: involvement of the colicin B receptor and of a citrate-inducible protein. J. Bacteriol. **127**:1370–1375.
19. **Hantke, K.** 1981. Regulation of ferric iron transport in *Escherichia coli* K-12: isolation of a constitutive mutant. Mol. Gen. Genet. **182**:288–292.
20. **Hantke, K.** 1984. Cloning of the repressor protein gene of iron-regulated systems in *Escherichia coli* K-12. Mol. Gen. Genet. **197**:337–341.
21. **Hawkes, R., E. Niday, and J. Gordon.** 1982. A dot-immunobinding assay for monoclonal and other antibodies. Anal. Biochem. **119**:142–147.
22. **Katz, E., and A. L. Demain.** 1977. The peptide antibiotics of *Bacillus*: chemistry, biogenesis, and possible functions. Bacteriol. Rev. **41**:449–474.
23. **Klebba, P. E., M. A. McIntosh, and J. B. Neilands.** 1982. Kinetics of biosynthesis of iron-regulated membrane proteins in *Escherichia coli*. J. Bacteriol. **149**:880–888.
24. **Laemmli, U. K.** 1970. Cleavage of structural proteins during the assembly of the head of bacteriophage T4. Nature (London) **227**:680–685.
25. **Laird, A. J., D. W. Ribbons, G. C. Woodrow, and I. G. Young.** 1980. Bacteriophage Mu-mediated gene transposition and in vitro cloning of the enterochelin gene cluster of *Escherichia coli*. Gene **11**:347–357.

26. **Laird, A. J., and I. G. Young.** 1980. Tn*5* mutagenesis of the enterochelin gene cluster of *Escherichia coli*. Gene **11**:359–366.
27. **Langman, L., I. G. Young, G. E. Frost, H. Rosenberg, and F. Gibson.** 1972. Enterochelin system of iron transport in *Escherichia coli*: mutations affecting ferric-enterochelin esterase. J. Bacteriol. **112**:1142–1149.
28. **Luke, R. K. J., and F. Gibson.** 1971. Location of three genes concerned with the conversion of 2,3-dihydroxybenzoate into enterochelin in *Escherichia coli* K-12. J. Bacteriol. **107**:557–562.
29. **Lundrigan, M. D., and R. J. Kadner.** 1986. Nucleotide sequence of the gene for the ferrienterochelin receptor FepA in *Escherichia coli*. J. Biol. Chem. **261**:10797–10801.
30. **Maniatis, T., E. F. Fritsch, and J. Sambrook.** 1982. Molecular cloning: a laboratory manual. Cold Spring Harbor Laboratory, Cold Spring Harbor, N.Y.
31. **McIntosh, M. A., and C. F. Earhart.** 1976. Effect of iron on the relative abundance of two large polypeptides of the *Escherichia coli* outer membrane. Biochem. Biophys. Res. Commun. **70**:315–322.
32. **McIntosh, M. A., and C. F. Earhart.** 1977. Coordinate regulation by iron of the synthesis of phenolate compounds and three outer membrane proteins in *Escherichia coli*. J. Bacteriol. **131**:331–339.
33. **Messing, J., and J. Vieira.** 1982. A new pair of M13 vectors for selecting either DNA strand of double-digested restriction fragments. Gene **19**:269–276.
34. **Miller, J. H.** 1972. Experiments in molecular genetics. Cold Spring Harbor Laboratory, Cold Spring Harbor, N.Y.
35. **Morgan, M. K., and A. K. Chatterjee.** 1985. Isolation and characterization of Tn*5* insertion mutants of *Pseudomonas syringae* pv. *syringae* altered in the production of the peptide phytotoxin syringotoxin. J. Bacteriol. **164**:14–18.
36. **Neilands, J. B.** 1982. Microbial envelope proteins related to iron. Annu. Rev. Microbiol. **36**:285–309.
37. **O'Brien, I. G., and F. Gibson.** 1970. The structure of enterochelin and related 2,3-dihydroxy-*N*-benzoylserine conjugates from *Escherichia coli*. Biochim. Biophys. Acta **215**:393–402.
38. **Pickett, C. L., L. Hayes, and C. F. Earhart.** 1984. Molecular cloning of the *Escherichia coli* K-12 *entACGBE* genes. FEMS Microbiol. Lett. **24**:77–80.
39. **Pierce, J. R., and C. F. Earhart.** 1986. *Escherichia coli* K-12 envelope proteins specifically required for ferrienterobactin uptake. J. Bacteriol. **166**:930–936.
40. **Pollack, J. R., and J. B. Neilands.** 1970. Enterobactin, an iron transport compound from *Salmonella typhimurium*. Biochem. Biophys. Res. Commun. **38**:989–992.
41. **Pugsley, A. P., and P. Reeves.** 1976. Characterization of group B colicin B-resistant mutants of *Escherichia coli* K-12: colicin resistance and the role of enterochelin. J. Bacteriol. **127**:218–228.
42. **Rigby, P. W. J., M. Dieckmann, C. Rhodes, and P. Berg.** 1977. Labeling deoxyribonucleic acid to high specific activity in vitro by nick-translation with DNA polymerase I. J. Mol. Biol. **113**:237–251.
43. **Sanger, F., S. Nicklen, and A. R. Coulson.** 1977. DNA sequencing with chain-terminating inhibitors. Proc. Natl. Acad. Sci. USA **74**:5463–5467.
44. **Shine, J., and L. Dalgarno.** 1974. The 3'-terminal sequence of *Escherichia coli* 16S ribosomal RNA: complementarity to nonsense triplets and ribosome binding sites. Proc. Natl. Acad. Sci. USA **71**:1342–1346.
45. **Soberon, X., L. Covarrubias, and F. Bolivar.** 1980. Construction and characterization of new cloning vehicles. IV. Deletion derivatives of pBR322 and pBR325. Gene **9**:287–305.
46. **Towbin, H., T. Staehelin, and J. Gordon.** 1979. Electrophoretic transfer of proteins from polyacrylamide gels to nitrocellulose sheets: procedure and some applications. Proc. Natl. Acad. Sci. USA **76**:4350–4354.
47. **Ullmann, A., D. Perrin, F. Jacob, and J. Monod.** 1965. Identification par complementation *in vitro* et purification d'un segment peptidique de la β-galactosidase d'*Escherichia coli*. J. Mol. Biol. **12**:918–923.
48. **Way, J. C., M. A. Davis, D. Morisato, D. E. Roberts, and N. Kleckner.** 1984. New Tn*10* derivatives for transposon mutagenesis and for construction of *lacZ* operon fusions by transposition. Gene **32**:369–379.
49. **Woodrow, G. C., I. G. Young, and F. Gibson.** 1975. Mu-induced polarity in the *Escherichia coli* K-12 *ent* gene cluster: evidence for a gene (*entG*) involved in the biosynthesis of enterochelin. J. Bacteriol. **124**:1–6.
50. **Woodrow, G. C., I. G. Young, and F. Gibson.** 1979. Biosynthesis of enterochelin in *Escherichia coli* K-12: separation of the polypeptides coded for by the *ent*D, E, F and G genes. Biochim. Biophys. Acta. **582**:145–153.
51. **Young, I. G., L. Langman, R. K. J. Luke, and F. Gibson.** 1971. Biosynthesis of the iron-transport compound enterochelin: mutants of *Escherichia coli* unable to synthesize 2,3-dihydroxybenzoate. J. Bacteriol. **106**:51–57.